Pergamon

Cement and Concrete Research 30 (2000) 191–196

CEMENT AND CONCRETE RESEARCH

Hexagonal ice in hardened cement

Erland M. Schulson[a,*], Ian P. Swainson[b], Thomas M. Holden[b], Charles J. Korhonen[c]

[a]*Thayer School of Engineering, Dartmouth College, Hanover, NH 03755, USA*
[b]*Chalk River Labs, Chalk River, Ontario K0J1J0, Canada*
[c]*Cold Regions Research & Engineering Lab, Hanover, NH 03755, USA*

Received 6 July 1999; accepted 8 November 1999

Abstract

Neutron diffraction from nearly saturated cement paste (made from D_2O, water/cement ratio = 0.36, hardened 3 months under lime-saturated D_2O) has shown that the pore water transformed mainly to hexagonal ice (Ih) upon slow cooling below the (bulk) equilibrium freezing point of heavy water (276.8°K). The amount of ice increased continuously upon cooling to 227°K, and then decreased continuously upon heating. At every temperature below 276.8°K, the ice content was greater upon heating than upon cooling. The results were used to calculate the pore size distribution, which ranged mainly between a diameter of 3 and 30 nm.

Keywords: Neutron diffraction; Crystal structure; Pore size distribution; Freeze/thaw

1. Introduction

Hardened Portland cement is a microporous material that is used to bind aggregate in concrete. When saturated with water and then thermally cycled to temperatures below and above the bulk freezing point, it cracks, due to the development of internal stresses induced by the freezing of pore water. Upon repeated cycling, the cracks grow and interact and lead eventually to macroscopic degradation and premature failure of concrete structures in cold regions. Marchand et al. [1] reviewed the problem. At root is the movement of pore water, either toward the centers of freezing and to the growth of ice lenses or away from the centers of freezing and to the development of hydraulic pressure. To better understand the thermodynamics of freezing and the mechanical behavior of the frozen composite, it is important to know the structure of the ice that forms within the confined spaces. Here we show for the first time, through a direct in situ neutron diffraction experiment, that the ice possesses the Ih crystal structure.

2. Methods

The material used in this study was prepared from Type II Portland cement and heavy water. The mass ratio of water to cement was 0.36. Heavy water (D_2O) was used instead of light water to reduce incoherent scattering. Cylindrical specimens (5 mm diameter, 50 mm length) were cast in a Plexiglas mold, allowed to harden for about 3 days, ejected, and then submerged under lime-saturated heavy water for 3 months at room temperature. Subsequently, they were encapsulated in vanadium tubes, purged with helium, and then irradiated with monochromatic thermal neutrons of 0.13286 nm wavelength (selected using a {531} reflection from a crystal of Si). Care was taken to ensure that the specimens were centered in the beam. The specimens were cooled from room temperature (298°K) to 227°K in increments of 5°K and then warmed to 298°K, within a liquid nitrogen cryostat. Care was also taken not to quench the samples on initial placement into the cryostat. A heating chamber was developed to ensure that the sample temperature did not drop below the bulk freezing point at the start of the experiment and to prevent the development of thermal gradients. The temperature was measured using two calibrated Si diodes placed within the tubes, and was accurate to ± 0.3°K. At each temperature, the specimens were irradiated for 3 h after equilibrating for 1.5 h. This exposure was determined from several preliminary cooling and heating trials using different specimens. The results presented here were obtained once the procedure had been established. They were obtained from one specimen subjected to one cycle of cooling and heating.

Data were obtained in terms of scattered intensity vs. diffraction angle 2θ (where θ is the Bragg angle), using the C2

* Corresponding author. Tel.: 603-646-2888; fax: 603-646-3856.
E-mail address: erland.schulson@dartmouth.edu (E. Schulson)

0008-8846/00/$ – see front matter
PII: S0008-8846(99)00229-X

spectrometer of Chalk River Labs NRU reactor. The angle 2θ ranged from 9 to 89° for each run at each temperature.

3. Results and analysis

3.1. Structure of ice

The diffraction pattern contained many lines due to the multiple phases present in a cement. The most significant change in the pattern was the emergence, upon cooling to temperatures below the equilibrium (bulk) freezing temperature of the (heavy) pore water D_2O (276.8°K), of two new, fairly strong low-angle peaks, at $2\theta = 19.7$ and 20.8°, as seen in Fig. 1. There was also some evidence of a third new line, albeit a weaker one, at $2\theta \sim 22°$. The intensity of the two stronger lines increased nearly continuously as the temperature decreased to 227°K, and then decreased nearly continuously as the temperature increased during the warming stage of the experiment, shown in Fig. 2. Both lines appeared to grow (upon cooling) and to shrink (upon heating) at about the same rate, suggesting that they originated from the same source.

To determine the origin of these new peaks, we simulated diffraction from both Ih and cubic ice (Ic). For Ih we used as lattice parameters (at 277°K) $a = 0.4526$ nm and $c = 0.7369$ nm; for Ic we used $a = 0.6381$ nm. We did not simulate diffraction from high-pressure forms of ice because they are stable only at pressures above about 200 MPa, which is at least one order of magnitude greater than the matrix of C-S-D (C = CaO, S = SiO_2, D = D_2O) can withstand. The Ih simulation yielded a triplet of peaks, at $2\theta = 19.5$, 20.8, and 22.0°, corresponding to diffraction from {1000},{0002} and $\{10\bar{1}0\}$, respectively. The Ic simulation gave a line at 20.8°, corresponding to diffraction from {111}. In other words, the first and third new peak are unique to Ih, while the second is common to both Ih and Ic.

Thus, on the basis of the simulations and on the observation that the two stronger lines grew *and* shrank together, we conclude that the new reflections originate predominantly from Ih. We also conclude that the ice formed mainly within the pores and not on the surface. Had a significant amount formed on the surface, it would have manifested itself through a rather sudden drop in the peak intensities upon heating near the bulk melting point due to the expul-

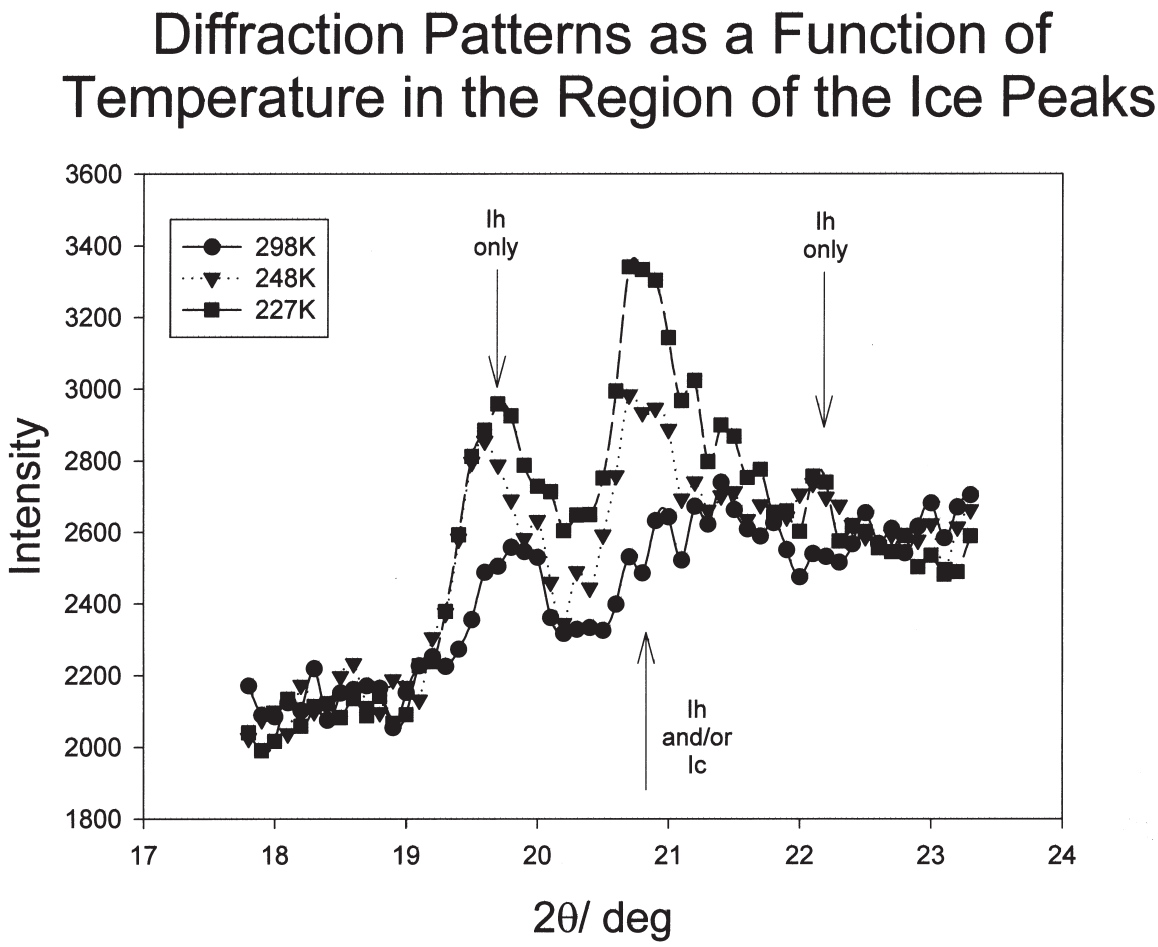

Fig. 1. Neutron diffraction patterns from nearly saturated hardened cement at 298, 248, and 227°K. Note the emergence of diffraction peaks at 19.7 and 20.8° (and possibly at 22°) upon cooling. Ih denotes hexagonal ice; Ic denotes cubic ice.

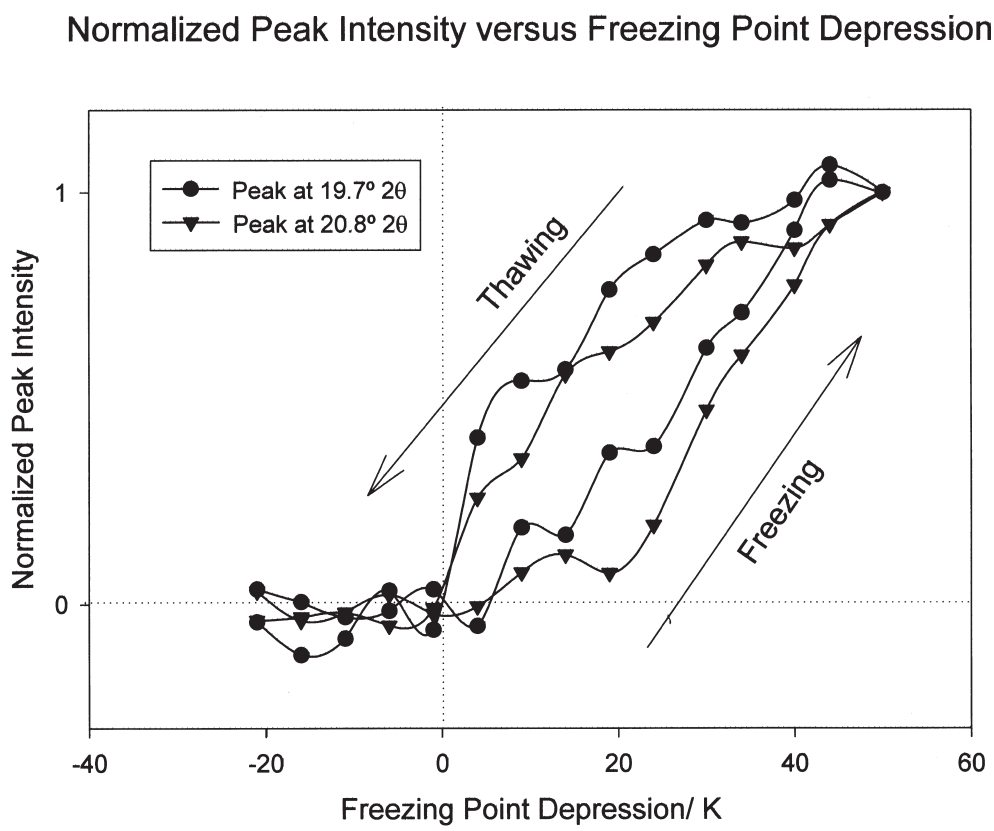

Fig. 2. Integrated intensities of the 19.7° peak (from 19.0 to 20.3°) and the 20.8° peak (from 20.3 to 21.6°) vs. temperature during cooling and heating. The normalized peak intensity was defined from the difference in counts at 227°K and the average background at 277°K and by normalizing to unity the difference at 227°K.

sion of pore water. Had Ic dominated within the pores, only the second line ($2\theta = 20.8°$) would have lost intensity upon heating. Low density amorphous (LDA) ice would exhibit a broad maximum near the Ih triplets. Thus, while we cannot conclude that Ic and LDA ice did not form at all, we can conclude that Ih is responsible for most of the changes in Bragg scattering due to freezing and thawing in this experiment.

Earlier work on the structure of ice formed within other microporous materials appears somewhat contradictory. Handa et al. [2] found from an X-ray diffraction study that pore water within both Vycor glass (8 nm average pore diameter) and silica gel SG20 (4 nm average pore diameter) transformed to Ih upon slowly cooling to 85°K, but formed Ic upon quenching in liquid nitrogen. Dunn et al. [3] found from a neutron diffraction study that heavy water within porous silica (9 nm average pore diameter) transformed to Ih when slowly cooled to 252°K, but formed mainly Ic at lower temperatures (242–213°K). Steytler et al. [4] reported from a neutron diffraction study that D_2O within microporous silica (9 nm average pore diameter) transformed to Ic when cooled to 258°K. They also noted a minor amount of Ih, and wondered whether that contribution came from ice on the free surface. Perhaps the structure of the surface of the pore is important in determining which phase forms, since there is very little energetic difference between Ic and Ih. Kinetics may also be a factor.

3.2. Pore size distribution

That ice formed nearly continuously upon cooling below the bulk freezing point of the pore water implies a distribution of freezing sites. We attribute this feature to the suppression of freezing caused by the ice/water interfacial energy (i.e., to the increase in chemical potential of ice with respect to water as the pore size decreases). This is an example of the Gibbs-Thompson effect: it has been considered at length by Everett [5] and more recently by Scherer [6], and was first used by Fagerlund [7] to determine pore size distribution in cellular concrete from freezing point depression. Accordingly, for spherically shaped pores of radius r_p the depression of the freezing point $\Delta T = T - T_0$ may be obtained from the relationship shown in Eq. (1) [8]:

$$\frac{1}{r_c} = \frac{f}{2\Gamma_{LS}} \int_{T_0}^{T} \frac{\Delta S_f}{V_L} dT \tag{1}$$

where r_c is the radius of the ice/water interface, Γ_{LS} is the ice/water interfacial energy, ΔS_f is the entropy of fusion, and V_L is the molar volume of the water; f is a shape factor whose value is 1 for spherical interfaces and 2 for cylindrical interfaces. From the assumption that the interface adopts a spherical shape during freezing and from measurements of solidification thermograms of water, Brun et al. [8] obtained

the following relationship for the radius of the pore, r_p, within which freezing is occurring [see Eq. (2)]:

$$r_p(nm) = -\frac{64.67}{\Delta T} + 0.57 \quad (2)$$

Eq. (2) incorporates the unbound water that lines the pore walls, whose thickness, δ, is assumed to be δ = 0.8 nm (i.e., about two monolayers). Thus, from the freezing-point depressions (see Fig. 3, cooling stage only), calculation indicates that the pores mainly ranged in size (diameter) from 3 to 30 nm, as seen in Fig. 4 In other words, it appears that the ice formed within gel pores of the C-S-D matrix. Capillary pores were largely absent, owing to the low water/cement ratio.

3.3. Freeze/thaw hysteresis

Although the amount of ice that formed was not determined, it was clear from the relative intensity of the diffraction peaks that at every temperature below 276.8°K there was more ice upon heating than upon cooling. Fig. 2 illustrates this point. The width of the hysteresis is 15 to 20°K over much of the temperature range investigated. This observation confirms earlier observations of hysteresis in hardened and saturated Portland cement detected using scanning calorimetry [9], and is similar to the hysteresis seen by Li et al. [10] in microporous Vycor via small angle neutron scattering. No water was observed to be expelled from the pores upon freezing in both the experiments of Li et al. and our own (we found no evidence for a large proportion of melting near 277°K), implying that the additional volume must have been taken up in the matrix, assuming that the material was nearly fully saturated.

In the microporous Vycor of Li et al. [10], much of the volume increase due to freezing was accommodated by densification of the silica framework. This notion reflects the fact, evident from inelastic neutron scattering [11,12], that silica glass, although macroscopically rather rigid, can be microscopically compliant on a local scale due to low-frequency or "floppy" modes of vibration that are intrinsic to the framework of SiO_4 tetrahedra. This mechanism, however, is unlikely to operate to the same degree in Portland cement: while the empty silica structure of Vycor is open to simple volume-changing distortions [12], the cation-filled structures of hardened cement would not be so accommo-

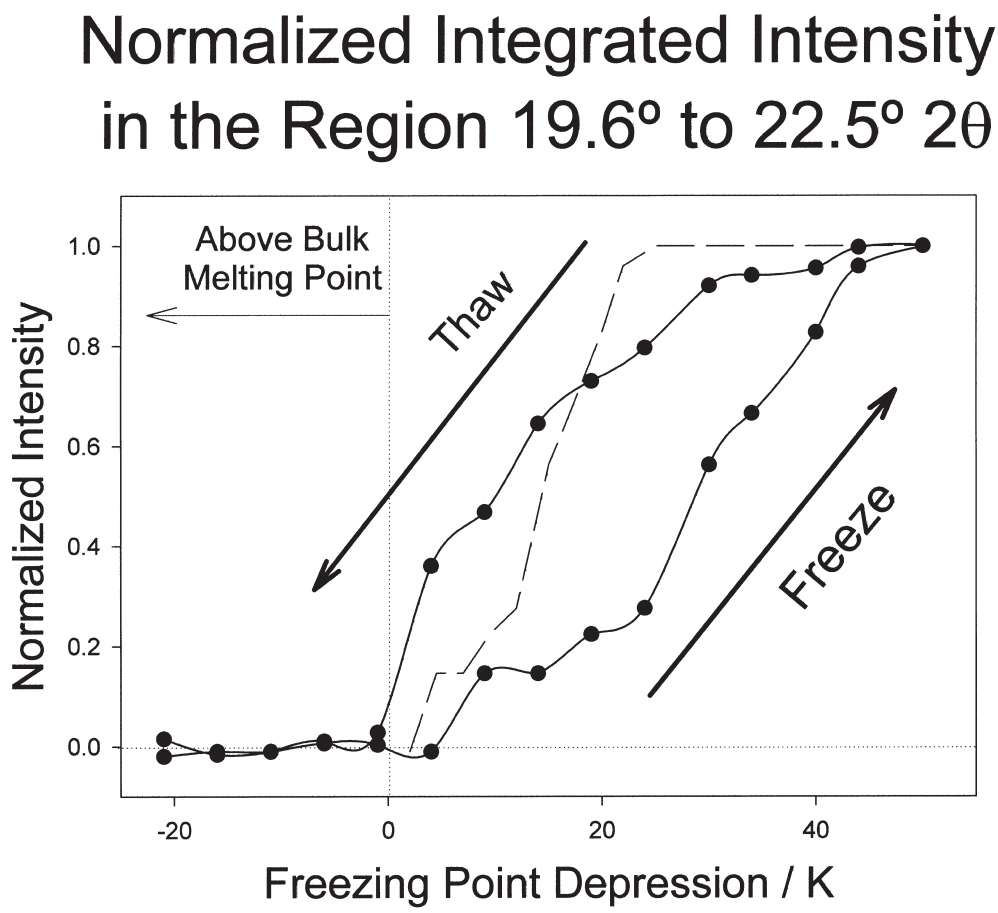

Fig. 3. Normalized Bragg intensity calculated from the ice peaks over the range from 19 to 22.5°. The background was corrected as with Fig. 2. The points show the intensities as a function of freezing and thawing. The dotted line represents the thawing curve calculated on the assumption of a cylindrical pore shape. This calculation uses the measured intensity changes on freezing as a function of depression temperature and Eqs. (3) and (4). The observed hysteresis clearly cannot be explained by a constant shape factor for all pores.

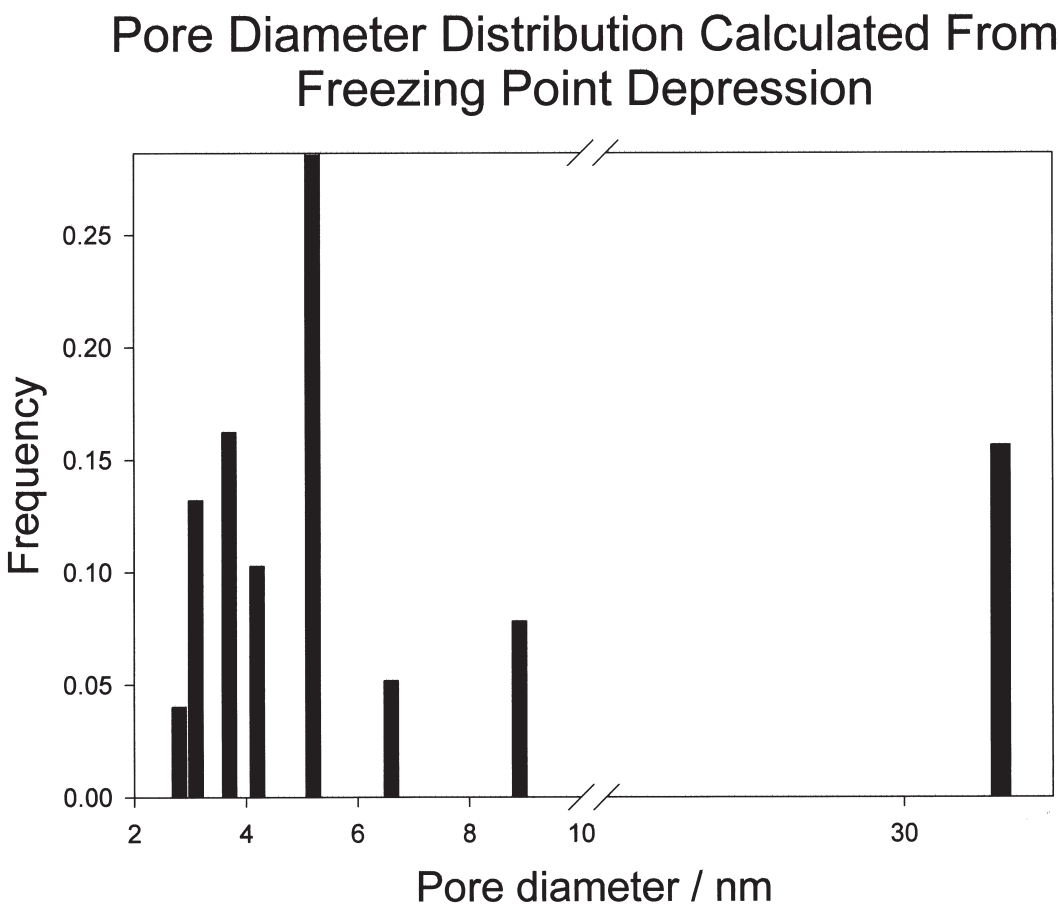

Fig. 4. Pore diameter distribution calculated using the data (averaged over both peaks) of Fig. 2 (cooling stage only).

dating. Instead, the pore walls may have cracked open, thereby lessening the degree to which the Gibbs-Thomson effect depressed the melting point. Another possibility [8] is that restrictions may have been at play (i.e., necks between pores may have controlled the freezing temperatures while the "true" pore size controlled melting, in which case the pore diameters calculated above would correspond more to neck size than to head size). The other explanation, following Brun et al. [8], considers the pores to be cylindrical in shape, and invokes differences in the shape factor *f*. Upon cooling, the ice/water interface is assumed to be hemispherical ($f = 1$) as already noted, and so the freezing-point suppression can be given by the relationship seen in Eq. (3) [8]:

$$\Delta T_{\text{cool}} = -\frac{64.67}{r_p - 0.57} \tag{3}$$

Upon heating, the interface is assumed to be cylindrical ($f = 2$) due to the pore being filled with ice, and so the suppression is reduced by a factor of two and may be given by the expression seen in Eq. (4) [8]:

$$\Delta T_{\text{heat}} = -\frac{32.33}{r_p - 0.68} \tag{4}$$

The pore radius r_p is given in nm. However, based upon the measured depression during freezing, this explanation overpredicts the observed hysteresis at lower temperatures and underpredicts the observed hysteresis at higher temperatures, as seen in Fig. 3. Shapes other than spheres and cylinders may account for these discrepancies.

It is noted that explanations based upon restrictions and shape factor imply that the amount of ice produced during cooling and warming is expected to be reversible upon further cycling. Damage, on the other hand, would shift the pore size distribution to larger sizes, leading to an irreversible effect and to more ice at a given temperature upon cooling through a subsequent cycle. More experiments are needed to examine these implications.

4. Conclusions

From neutron diffraction experiments on hardened cement paste of water/cement ratio = 0.36 nearly saturated with heavy water and cooled from 298 to 227°K and then warmed to 298°K, it is concluded that:

1. Ice formed upon cooling below the equilibrium (bulk) freezing point of 276.8°K;
2. the ice formed nearly continuously, implying a range of freezing sites; and

3. at any temperature below the bulk freezing point there was more ice upon heating than cooling, indicating freeze-thaw hysteresis.

Acknowledgments

We acknowledge Drs. R.A. Livingston and D. Klug and Profs. V. Penttala, G.W. Scherer, and E.J. Sellevold for helpful discussions. We also acknowledge the work of Ron Donaberger in developing the specialized cell for the experiment. This work was supported by a grant from USA-CRREL through support from U.S. Federal Highway Administration.

References

[1] J. Marchand, R. Pleau, R. Gagne, Deterioration of concrete due to freezing and thawing, in: J. Skalny, S. Mindess (Eds.), Materials Science of Concrete IV, The American Ceramic Society, Websterville, Ohio, 1995, pp. 283–354.

[2] Y.P. Handa, M. Zakrzewski, C. Fairbridge, Effect of restricted geometries on the structure and thermodynamic properties of ice, J Phys Chem 96 (1992) 8594–8599.

[3] M. Dunn, J.C. Dore, P. Chieux, Structural studies of ice formation in porous silicas by neutron diffraction, J Crystal Growth 92 (1988) 233–238.

[4] D.C. Steytler, J.C. Dore, C.J. Wright, Neutron diffraction study of cubic ice in a porous silica network, J Phys Chem 87 (1983) 2458–2459.

[5] D.H. Everett, The thermodynamics of frost damage to porous solids, Trans Faraday Soc 57 (1961) 1541–1551.

[6] G.W. Scherer, Crystallization in pores, Cem Concr Res 29 (1999) 1347–1358.

[7] G. Fagerlund, Determination of pore-size distribution from freezing-point depression, Matériaux et Constructions 33 (1973) 215–225.

[8] M. Brun, A. Lallemand, J.-F. Quinson, C. Eyraud, A new method for the simultaneous determination of the size and shape of pores: The thermoporometry, Thermochimica Acta 21 (1977) 59–88.

[9] O.S. DeFontenay, E.J. Sellevold, Ice formation in hardened cement paste—I. Mature water saturated pastes, in: Durability of Building Materials and Components, ASTM STP 691, 1980.

[10] J.-C. Li, D.K. Ross, M.J. Benham, Small-angle neutron scattering studies of water and ice in porous Vycor glass, J Appl Cryst 24 (1991) 794–802.

[11] I.P. Swainson, M.T. Dove, Low-frequency floppy modes in β-cristobalite, Phys Rev Lett 71 (1993) 193–196.

[12] M.T. Dove, M.J. Harris, A.C. Hannon, J.M. Parker, I.P. Swainson, I.P.M. Gambhir, Floppy modes in crystalline and amorphous silicates, Phys Rev Lett 78 (1997) 1070–1073.